

Air entrainment in spray jets

S. A. MacGregor

School of Mechanical Engineering, University of Bath, Bath, UK

The entrainment of air into spray jets has been considered. Measurements have been made of the air entrainment into spray jets and compared with the results of a simple model of air entrainment. Comparison of the results from free air jet experiments with that from sprays indicate that a free air jet is able to entrain as much as 50 times more fluid than its spray counterpart over a similar length.

Keywords: entrainment; jets; two-phase flow

Introduction

The behavior of sprays and how they interact with their surroundings is of interest in many areas. Particle-induced entrainment is especially important in combustion systems, such as furnaces, gas turbines, and diesel engines. However, the importance of sprays is not only limited to combustion systems. There are many other processes in which entrainment can be an important parameter, e.g., two-phase flows of solid particles or liquid droplets in gas and spray processes in industrial or food-processing applications. The influence that a spray is able to exert on its surroundings may have a significant effect on the effectiveness and efficiency of the process.

Consider the processes that occur in a direct-injection diesel during fuel injection. Many analyses of sprays in this situation assume that the droplets in the spray evaporate instantaneously and that the jet may therefore be treated as a single-phase gas jet. An example of this treatment is the water-analogy experiments used to study the in-cylinder flow in direct-injection diesel engines.¹ The flow at the point of injection is studied using a water model. This allows the process to be studied on a time scale much greater than that encountered in an actual diesel engine. In the water-analogy experiment, it is assumed that particles evaporate so rapidly that the jet may be assumed to be single phase. The assumption that small particles evaporate rapidly is valid, but larger particles will have evaporation times of the same order of magnitude as the mixing times, and may in some cases be much longer.² In experiments,³ kerosene droplets of 100 μm were found to take a significant time to heat up in an atmosphere maintained constant at 1000 K. In applications where the particles are larger, the times will increase, and thus particles moving through a flow field may influence the surrounding fluid. In applications such as coal-fired diesel engines,⁴ the time for combustion of fuel particles may be significant in comparison with the mixing times involved.

In flows where the evaporation times are of the same order as the mixing times, the entrainment of air from the surroundings will have a significant effect on the combustion of fuel droplets or particles, a process which will be controlled by the mixing rate. The level of entrainment may have a significant effect on the local stoichiometry of the flow. This will in turn have a significant effect on the performance and emission levels of a combustion system. This will be especially important in the early stages of jet development, where many particles will not

have evaporated. The importance of entrainment is not only limited to combustion problems. It may have considerable influence on the flow field in many processes that involve two-phase flow, either solid particles or liquid droplets in gas.

There have been many articles published on single-phase jets, some of which^{5,6} have studied the entrainment of fluid into free jets. In these, entrainment constants have been generated that relate the mass entrainment to the axial distance downstream from the point of injection. The mass flow rate in the jet was found to increase linearly with distance downstream from the point of injection.⁵ This may be expressed in the form

$$\frac{\dot{m}_t}{\dot{m}_i} = K \left(\frac{x}{d} \right) \quad (1)$$

where K is the entrainment constant and \dot{m} the mass flow rate. Typical values for the entrainment constant are of the order of 0.3.⁵

Much of the work that has considered sprays has concentrated in the area of particle generation and size distributions. Measurements of particle velocity have been made using laser Doppler anemometry.⁷ The aim of the present study is to consider the entrainment of air into spray jets. The experimental data have been compared with the results of a simple model of air entrainment.

Procedure

Experimental

Experimental data were gathered using a method proposed by Ricou and Spalding,⁶ which measured the total mass of fluid entrained into the jet. This eliminated the need to measure the velocity profiles in the jet. The arrangement for the experiment is shown in Figure 1. The jet is completely enclosed, and the supply of entrainable air was controlled such that the pressure in the enclosure matched that of the surrounding atmosphere.

The initial experiments were performed using a nozzle in which it was easy to vary the geometry of the jet (nozzle A, figure 1). This was achieved by varying the size of the orifice. The nozzle gave a reasonably wide range of mass flow rates, and the droplets produced by this arrangement were rather large, typically of the order of 500–1000 μm . Data were also collected from a nozzle that generated a spray with a much smaller mean particle size, typically of the order of > 100 μm (nozzle B).

Theoretical considerations

A simple model of the entrainment was developed to compare with the experimental data. The model makes a number of basic assumptions, which are listed below.

Address reprint requests to Dr. MacGregor at the School of Mechanical Engineering, University of Bath, Bath, UK.

Received 13 November 1989; accepted 4 January 1991

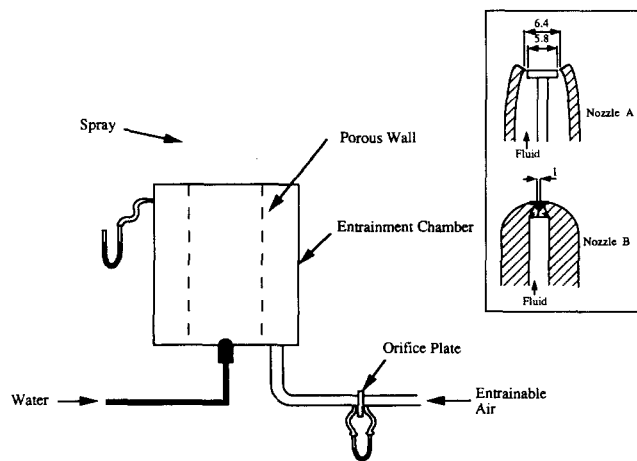


Figure 1 Schematic diagram of experimental apparatus

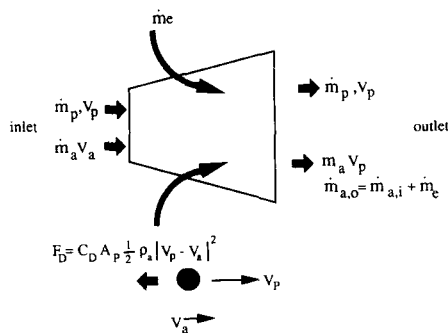


Figure 2 Entrainment model

- (1) The momentum in the jet is conserved, which may be expressed as

$$\sum_{j=1}^B (\dot{m}_{i,p_j} V_{i,p_j} + \dot{m}_{i,a_j} V_{i,a_j}) + \sum_{j=1}^B (\dot{m}_{o,p_j} V_{o,p_j} + \dot{m}_{o,a_j} V_{o,a_j}) = 0 \quad (2)$$

- (2) The particle velocity is reduced by drag forces exerted by the surrounding fluid. The drag force is given by

$$F_D = C_D A_p \frac{1}{2} \rho_a V^2 \quad (3)$$

where $V = V_a - V_p$ is the difference between the particle and the local air velocity. The area A_p is the projected area of the particle under consideration.

- (3) The only air motion is that within the confines of the spray.
- (4) The jet is assumed to break up after a set length.

A schematic diagram of the model is shown in Figure 2. In addition to the assumptions listed above, it was also necessary to assume divergence angles for the jet and also the particle size distributions generated by the nozzle. With nozzle A, it was possible to control the divergence of the jet to some degree. This parameter was not considered to be a significant parameter in this study and was maintained constant at approximately 25° . In the case of nozzle B, the divergence of the jet was set at a constant value of 30° .

The actual particle size distribution was unknown, and thus a distribution was assumed and generated using the Rosin-Rammler size distribution:⁸

$$R = \exp\left(-\left(\frac{d}{d_m}\right)^n\right) \quad (4)$$

where R is the fraction below size d . Experimental data were obtained for the effect of inlet mass flow and were compared with results from the simple model proposed above. Then the model was also used to assess the effects of a number of parameters that influence air entrainment. The parameters considered were

- (1) mass flow rate;
- (2) mean particle size;
- (3) size distributions.

Results

Effect of mass flow rate

Experiment

Experimental data for the variation of entrainment with mass flow rate is shown in Figure 3; data is included for both nozzles A and B, shown in Figure 1. In each case, entrainment rates are measured for jet lengths equivalent to approximately 70 inlet nozzle diameters. For nozzle A, the mass flow rate of the entrained air increases linearly with increasing mass flow rate. As the mass flow rate of the incoming flow increases, the particle velocities increase. The increased velocity results in a greater drag being exerted on the particles, and therefore the particles experience more rapid decelerations, which result in more energy being transferred from the particles to the surrounding fluid. The gradient of the line would suggest that there is a critical mass flow rate before which there is no significant breakup of the jet, and thus little or no entrainment occurs. In the case of nozzle A, this is approximately 0.13 kg s^{-1} of water, a figure obtained by extrapolation.

Notation

A	Area
B	Number of size bands in particle size distribution
C_D	Drag coefficient
d	Diameter
F_D	Drag force
K	Entrainment constant
m	Mass flow rate
n	Spread of Rosin-Rammler distribution
R	Fraction below given size
V	Velocity
X	Axial distance

Greek symbols

ρ Density

Subscripts

a	Air
e	Entrained
i	Inlet
m	Mean
o	Outlet
p	Particle
s	Surrounding fluid
t	Total

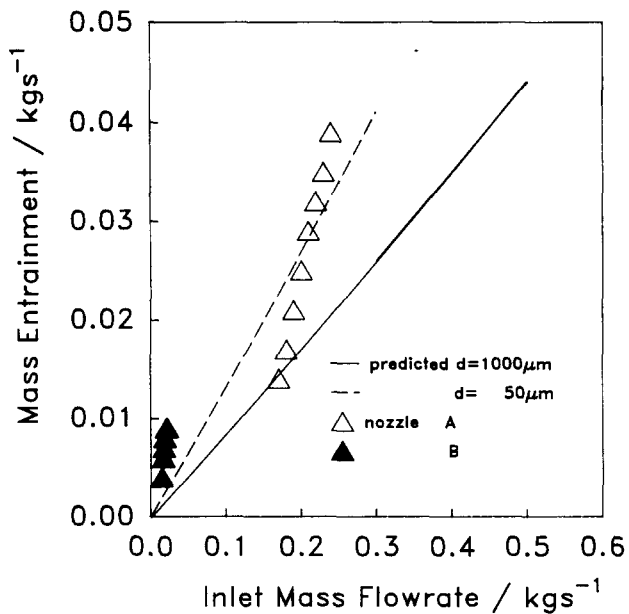


Figure 3 Variation of mass entrainment with inlet mass flow rate

The data from nozzle B show a similar linear variation to nozzle A. However, the range of flow rate is much reduced due to the sizes of the respective nozzles. The gradient of the two curves would appear to be much too great to reflect only the increasing mass flow rate at inlet. As the inlet mass flow rate increases, there is evidence that the mean diameter of the particles is reduced. The increased mass flow rate gives rise to a much more efficient atomization process, especially in the case of nozzle A, although this effect has yet to be quantified. As the particle size is reduced, the energy of the particles is more readily transferred to the surrounding fluid and thus more air is entrained. In the case of nozzle B, the particle size distribution does not vary greatly with changing mass flow rate. The smaller particles experience much greater decelerations than do the large particles, due to the greater surface area for a given mass of fluid, and thus they have a tendency to entrain more fluid. In the experimental results, it is reasonable to assume that a mass flow rate will be reached beyond which further increases will result in no further changes in the spray pattern.

Prediction

Shown in Figure 3 together with the experimental data are results of predictions of the variation of mass entrainment with inlet mass flow rate. The entrained mass flow rate increases linearly with increasing inlet mass flow rate. The curve for a mean particle size of $50 \mu\text{m}$ has a steeper gradient than that for the case with a mean particle size of $100 \mu\text{m}$. This variation is in agreement with the conclusions drawn from the experimental data described above.

On first inspection of the data, the experimental results do not agree particularly closely with the predicted data. This is really due to the simplicity of the model. The model makes no allowance for the breakup mechanism, which is a function of nozzle geometry; a constant particle size distribution is assumed for the range of flow rates considered.

Considering the obvious simplicity of the theory, the predictions do give entrainment rates that are of the same order of magnitude as the experimental data. The model was used to assess the effect of the parameters, which were not possible to

measure, on the entrainment of air into the jet. These parameters were mean particle size, particle size distribution, and the spread of the size distribution.

Variation of mass entrainment with length

Experiments with free air jets⁵ show that the mass flow rate in the jet increases linearly with distance downstream from the point of injection.⁶ The entrainment rate is constant along the length of the jet.⁵ The equivalent plot is shown in Figure 4 for spray jets. The data presented are predicted values. Only the entrained mass flow rate rather than the more usual total mass flow rate is presented, because the entrained mass flow rate is small by comparison with the inlet mass flow rate, due to the difference in density. For similar reasons, the actual mass flow rate rather than a nondimensional value is plotted. In the case of sprays, the variation is again linear. However, the linearity of these curves is coincidental and is dependent on the mean diameter of the particle in the spray, as will be seen in the next section. The mean particle diameter for the plots shown in Figure 4 is $1000 \mu\text{m}$, since this was representative of the particles generated by the nozzle A used in the experiment.

Effect of mean particle size

In Figure 5, the effect of mean particle size on the mass entrainment is shown. For large particle sizes, $d_m = 1000 \mu\text{m}$, the variation is linear. Also plotted in Figure 5 are some experimental data, obtained from nozzle A, for an inlet mass flow rate of 0.2 kg s^{-1} ; the mean particle size is in the range $500\text{--}1000 \mu\text{m}$ and shows reasonable agreement with the predicted values. As the mean size of the particles is reduced, so the entrainment rate along the length of the jet is no longer constant. The velocity of the particles is reduced as they move downstream, and eventually the velocity becomes so small that the particles are unable to entrain significant quantities of air. At this point the jet will probably behave in a manner similar to a single-phase jet, but the additional fluid entrained will be relatively small due to the low velocities in this region of the flow.

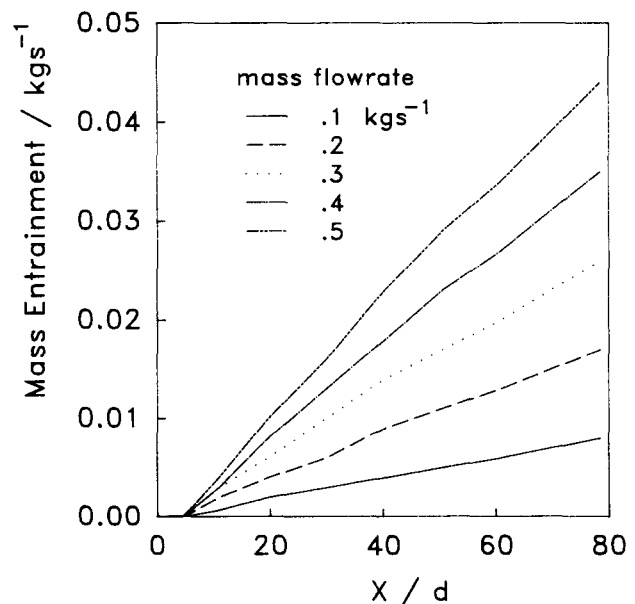


Figure 4 Effect of mass flow rate on entrainment along the length of the jet

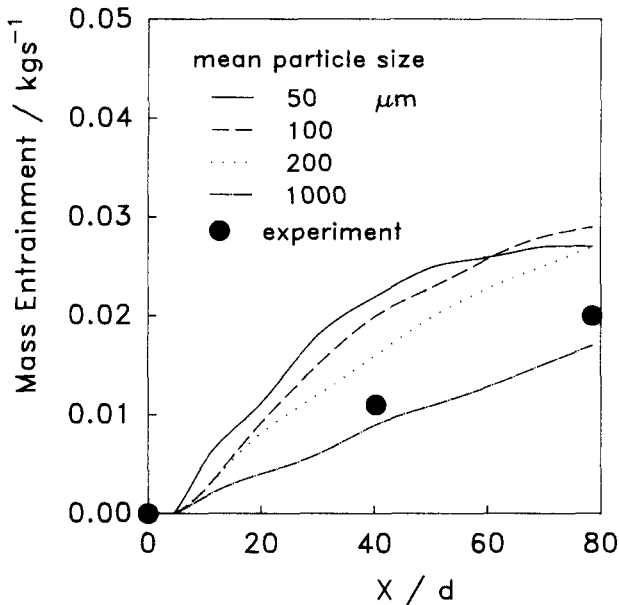


Figure 5 Effect of mean particle size on entrainment

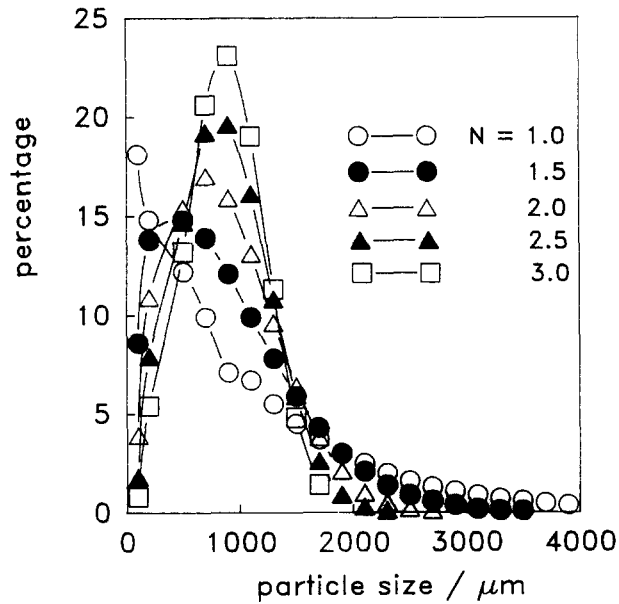


Figure 6 Particle size distributions

The variation of entrainment rate along the length of the jet may be explained by considering the particle dynamics. The small particles experience much greater decelerations than the large particles and thus they entrain more fluid, especially in the initial phases of the jet development where the velocities are high. Further downstream they have little energy left to induce entrainment, and thus the rate of entrainment decays until the local entrainment rate becomes zero. This effect is clearly seen in Figure 5. A similar variation will apply to the large particles but the velocity decay will not be so rapid; this explains the linear appearance of the curve for $X/d < 70$, for $d_m = 1000 \mu\text{m}$.

Effect of particle size distribution

As in the previous cases, the particle size distributions were generated using a Rosin-Rammler distribution⁸ as given in

Equation 4. By varying the constant n in this equation, it was possible to produce size distributions with varying degrees of spread. The size distributions considered are shown in Figure 6. The mean particle size is $1000 \mu\text{m}$.

The variation of entrainment along the length of the jet is approximately linear as was seen previously in Figure 4. The effect of the variation of the size distribution is shown in Figure 7. As the spread of the distribution increases, there is some evidence of variation in the entrainment rate, but not to a significant degree. This effect may be more in evidence at smaller mean diameters.

When the size distribution has a wide variation about the mean value, the mass entrainment increases slightly. This is due to the presence of smaller particles, which have a tendency to entrain larger quantities of fluid compared with the large particles. However, the overall entrainment is still dominated by the larger particles.

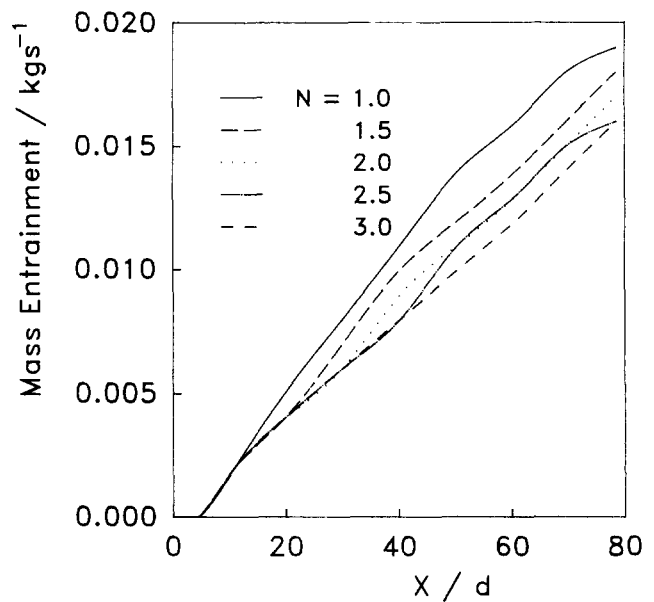


Figure 7 Effect of particle size distribution on entrainment

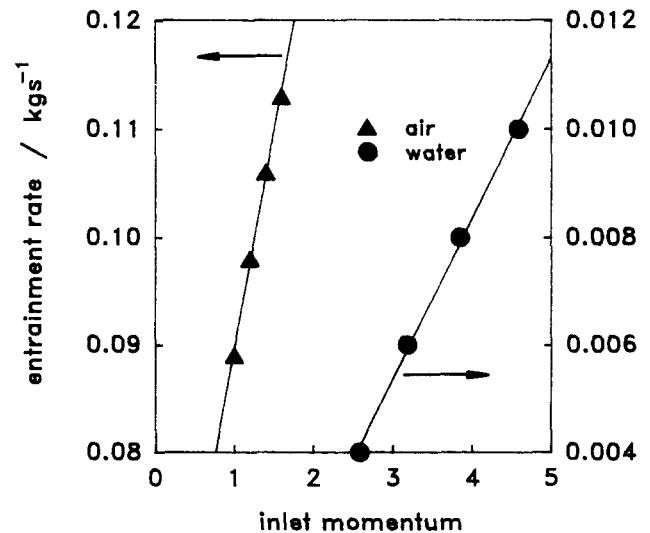


Figure 8 Variation of total mass entrainment with inlet momentum

Entrainment constants

In the case of air jets, the mass flow rate in the jet is related to the distance downstream from the nozzle by the relationship given in Equation 1. The entrainment constant, K , is typically of the order of 0.3. Clearly the relationship is linear. The entrainment is constant along the length of the jet. In the case of sprays, the entrainment is not always constant along the length of the jet. This is evident in the cases where the particle size distributions have small mean diameters. For the purpose of comparison, the entrainment constants for sprays have been calculated for a length of 70 nozzle diameters. In the case of the spray, it is necessary to take the density of the fluid in the jet into account, and so Equation 1 becomes⁶

$$\frac{\dot{m}_t}{\dot{m}_i} = K \left(\frac{X}{d} \right) \left(\frac{\rho_s}{\rho_i} \right)^{1/2} \quad (5)$$

This gives a value of the entrainment constant, K , of the order of 0.4 for sprays. The density ratio becomes dominant in this expression, and so it is relatively insensitive to changes in mass entrainment. It is more informative to compare the actual mass flow rates entrained by sprays and air jets. Taking jets of similar inlet momentum, the air jet is able to entrain much greater quantities than is possible in a spray. Figure 8 shows the mass entrainment for a range of inlet momentum for both spray and air jets. The data for the spray are based on the same length ratio as the air jet, i.e., $X/d=15$. It is clear that the air entrainment into the air jet is much greater than that of a spray. The air entrainment rate is typically of the order of 50 times greater in the case of air jets compared with sprays of similar inlet momentum.

Conclusions

The results of some preliminary tests have been presented, in which the entrainment of air into a spray jet has been considered. The results have been compared with the results of a

simple model based on some very basic assumptions. Although agreement is somewhat limited, the model was used to assess various parameters that influence air entrainment into sprays.

The most important parameter affecting entrainment is mass flow rate. The air entrained increases linearly with increasing mass flow rate for particle size distributions with relatively large mean sizes. The other important parameter is mean particle size, which affects the variation of entrainment rate along the length of the jet. The entrainment process appears to be relatively insensitive to the spread of the particle distribution, although in size distributions that exhibit a wide range of particle sizes this factor may become significant.

Comparing the level of entrainment in spray jets with that of single-phase injection processes would suggest that the spray is not very efficient in terms of generating entrainment. The introduction of a spray would have little effect on the bulk flow field into which it was injected.

References

- 1 Iduom, A., Wallace, F. J., Charlton, S. J., and Packer, J. P. An experimental and analytical study of jet impingement in high swirl D.I. diesel engines using the hydraulic analogy, SAE Paper 850263, 1985
- 2 Vranos, A. Turbulent mixing and NOX in gas turbines. *Combustion Flame*, 1974, **22**, 253–258
- 3 Chin, J. S., Durrett, R., and Lefebvre, A. H. The interdependence of spray characteristics and evaporation history of fuel spray. *ASME: J. Eng. Gas Turbines Power*, 1984, **106**, 639–644
- 4 Flynn, P. L., Hsu, B. D., and Leonard, G. L. Coal fueled diesel engine progress at GE transportation. *ASME: J. Eng. Gas Turbines Power*, 1990, **112**, 369–375
- 5 Hill, B. J. Measurement of local entrainment rate in the region of axisymmetric turbulent air jets. *J. Fluid Mech.*, 1972, **51**, 773–779
- 6 Ricou, F. P. and Spalding, D. B. Measurements of entrainment by axisymmetric turbulent jets. *J. Fluid Mech.*, 1961, **11**, 21–32
- 7 Hiroyasu, H. and Kadota, T. Fuel droplet size distribution in diesel chamber combustion, SAE Paper 740715, 1974
- 8 Rosin, P. and Rammler, E. The laws governing the fineness of powdered coal. *J. Inst. Fuel*, 1933, **7**, 29–36